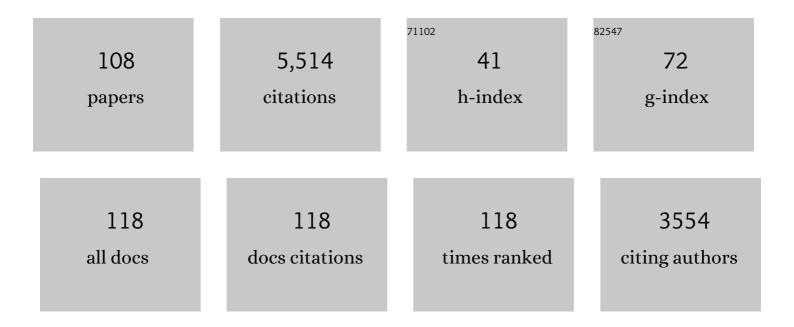
List of Publications by Year in descending order

Source: https://exaly.com/author-pdf/3926634/publications.pdf Version: 2024-02-01



ANNE MANCENEY

#	Article	IF	CITATIONS
1	Spreading of a granular mass on a horizontal plane. Physics of Fluids, 2004, 16, 2371-2381.	4.0	279
2	Ocean wave sources of seismic noise. Journal of Geophysical Research, 2011, 116, .	3.3	246
3	Frictional velocity-weakening in landslides on Earth and on other planetary bodies. Nature Communications, 2014, 5, 3417.	12.8	224
4	Erosion and mobility in granular collapse over sloping beds. Journal of Geophysical Research, 2010, 115, .	3.3	200
5	An Automatic Kurtosis-Based P- and S-Phase Picker Designed for Local Seismic Networks. Bulletin of the Seismological Society of America, 2014, 104, 394-409.	2.3	171
6	On the use of Saint Venant equations to simulate the spreading of a granular mass. Journal of Geophysical Research, 2005, 110, .	3.3	161
7	Granular and particle-laden flows: from laboratory experiments to field observations. Journal Physics D: Applied Physics, 2017, 50, 053001.	2.8	146
8	Numerical modeling of self-channeling granular flows and of their levee-channel deposits. Journal of Geophysical Research, 2007, 112, .	3.3	145
9	Slope instabilities in Dolomieu crater, Réunion Island: From seismic signals to rockfall characteristics. Journal of Geophysical Research, 2011, 116, .	3.3	137
10	A new Savage–Hutter type model for submarine avalanches and generated tsunami. Journal of Computational Physics, 2008, 227, 7720-7754.	3.8	136
11	A new model of Saint Venant and Savage–Hutter type for gravity driven shallow water flows. Comptes Rendus Mathematique, 2003, 336, 531-536.	0.3	121
12	Analytical Solution for Testing Debris Avalanche Numerical Models. Pure and Applied Geophysics, 2000, 157, 1081-1096.	1.9	118
13	Sinuous gullies on Mars: Frequency, distribution, and implications for flow properties. Journal of Geophysical Research, 2010, 115, .	3.3	118
14	Results of Back-Analysis of the Propagation of Rock Avalanches as a Function of the Assumed Rheology. Rock Mechanics and Rock Engineering, 2008, 41, 59-84.	5.4	117
15	Viscoplastic modeling of granular column collapse with pressure-dependent rheology. Journal of Non-Newtonian Fluid Mechanics, 2015, 219, 1-18.	2.4	116
16	Avalanche mobility induced by the presence of an erodible bed and associated entrainment. Geophysical Research Letters, 2007, 34, .	4.0	113
17	A Roe-type scheme for two-phase shallow granular flows over variable topography. ESAIM: Mathematical Modelling and Numerical Analysis, 2008, 42, 851-885.	1.9	111
18	Numerical modeling of landquakes. Geophysical Research Letters, 2010, 37, .	4.0	110

ANNE MANGENEY

#	Article	IF	CITATIONS
19	Numerical modeling of the Mount Steller landslide flow history and of the generated long period seismic waves. Geophysical Research Letters, 2012, 39, .	4.0	108
20	Modelling long-term seismic noise in various environments. Geophysical Journal International, 2012, 191, 707-722.	2.4	104
21	Fundamental changes of granular flow dynamics, deposition, and erosion processes at high slope angles: Insights from laboratory experiments. Journal of Geophysical Research F: Earth Surface, 2014, 119, 504-532.	2.8	100
22	Automated identification, location, and volume estimation of rockfalls at Piton de la Fournaise volcano. Journal of Geophysical Research F: Earth Surface, 2014, 119, 1082-1105.	2.8	94
23	On new erosion models of Savage–Hutter type for avalanches. Acta Mechanica, 2008, 199, 181-208.	2.1	87
24	Modelling secondary microseismic noise by normal mode summation. Geophysical Journal International, 2013, 193, 1732-1745.	2.4	86
25	Simulation of Tsaoling landslide, Taiwan, based on Saint Venant equations over general topography. Engineering Geology, 2009, 104, 181-189.	6.3	79
26	Exact solution for granular flows. International Journal for Numerical and Analytical Methods in Geomechanics, 2013, 37, 1408-1433.	3.3	76
27	Mobility and topographic effects for large Valles Marineris landslides on Mars. Geophysical Research Letters, 2007, 34, .	4.0	75
28	The effect of the earth pressure coefficients on the runout of granular material. Environmental Modelling and Software, 2007, 22, 1437-1454.	4.5	71
29	Numerical modeling of the Mount Meager landslide constrained by its force history derived from seismic data. Journal of Geophysical Research: Solid Earth, 2015, 120, 2579-2599.	3.4	71
30	A two-phase two-layer model for fluidized granular flows with dilatancy effects. Journal of Fluid Mechanics, 2016, 801, 166-221.	3.4	67
31	On the run-out distance of geophysical gravitational flows: Insight from fluidized granular collapse experiments. Earth and Planetary Science Letters, 2011, 311, 375-385.	4.4	65
32	Friction weakening in granular flows deduced from seismic records at the Soufrière Hills Volcano, Montserrat. Journal of Geophysical Research: Solid Earth, 2015, 120, 7536-7557.	3.4	59
33	Dynamic pore-pressure variations induce substrate erosion by pyroclastic flows. Geology, 2013, 41, 1107-1110.	4.4	58
34	On the shaping factors of the secondary microseismic wavefield. Journal of Geophysical Research: Solid Earth, 2015, 120, 6241-6262.	3.4	53
35	Simulation of water waves generated by a potential debris avalanche in Montserrat, Lesser Antilles. Geophysical Research Letters, 1998, 25, 3697-3700.	4.0	52
36	Continuum viscoplastic simulation of a granular column collapse on large slopes: <i>μ</i> ( <i>I</i> ) rheology and lateral wall effects. Physics of Fluids, 2017, 29, .	4.0	52

#	Article	IF	CITATIONS
37	Anisotropic behavior of GRIP ices and flow in Central Greenland. Earth and Planetary Science Letters, 1998, 154, 307-322.	4.4	51
38	Greenland under changing climates: sensitivity experiments with a new three-dimensional ice-sheet model. Annals of Glaciology, 1995, 21, 1-7.	1.4	48
39	Influence of the scar geometry on landslide dynamics and deposits: Application to Martian landslides. Journal of Geophysical Research, 2011, 116, .	3.3	46
40	Landslide boost from entrainment. Nature Geoscience, 2011, 4, 77-78.	12.9	46
41	A two-phase shallow debris flow model with energy balance. ESAIM: Mathematical Modelling and Numerical Analysis, 2015, 49, 101-140.	1.9	46
42	A numerical study of anisotropic, low Reynolds number, free surface flow for ice sheet modeling. Journal of Geophysical Research, 1997, 102, 22749-22764.	3.3	43
43	Isothermal flow of an anisotropic ice sheet in the vicinity of an ice divide. Journal of Geophysical Research, 1996, 101, 28189-28204.	3.3	41
44	Characterization of rockfalls from seismic signal: Insights from laboratory experiments. Journal of Geophysical Research: Solid Earth, 2015, 120, 7102-7137.	3.4	41
45	A multilayer shallow model for dry granular flows with the -rheology: application to granular collapse on erodible beds. Journal of Fluid Mechanics, 2016, 798, 643-681.	3.4	41
46	2D granular flows with the μ(I) rheology and side walls friction: A well-balanced multilayer discretization. Journal of Computational Physics, 2018, 356, 192-219.	3.8	38
47	Highâ€resolution bathymetry reveals contrasting landslide activity shaping the walls of the Midâ€Atlantic Ridge axial valley. Geochemistry, Geophysics, Geosystems, 2013, 14, 996-1011.	2.5	37
48	LiDAR derived morphology of the 1993 Lascar pyroclastic flow deposits, and implication for flow dynamics and rheology. Journal of Volcanology and Geothermal Research, 2012, 245-246, 81-97.	2.1	36
49	Estimation of dynamic friction of the Akatani landslide from seismic waveform inversion and numerical simulation. Geophysical Journal International, 2016, 206, 1479-1486.	2.4	34
50	Estimation of dynamic friction and movement history of large landslides. Landslides, 2018, 15, 1963-1974.	5.4	34
51	The dynamic response of prone-to-fall columns to ambient vibrations: comparison between measurements and numerical modelling. Geophysical Journal International, 2017, 208, 1058-1076.	2.4	33
52	An energy-consistent depth-averaged Euler system: Derivation and properties. Discrete and Continuous Dynamical Systems - Series B, 2015, 20, 961-988.	0.9	32
53	The shallow ice approximation for anisotropic ice: Formulation and limits. Journal of Geophysical Research, 1998, 103, 691-705.	3.3	31
54	Numerical simulation of the 30–45Âka debris avalanche flow of Montagne Pelée volcano, Martinique: from volcano flank collapse to submarine emplacement. Natural Hazards, 2017, 87, 1189-1222.	3.4	31

#	Article	IF	CITATIONS
55	Modeling of partial dome collapse of La Soufrière of Guadeloupe volcano: implications for hazard assessment and monitoring. Scientific Reports, 2019, 9, 13105.	3.3	31
56	Model Space Exploration for Determining Landslide Source History from Long-Period Seismic Data. Pure and Applied Geophysics, 2015, 172, 389-413.	1.9	29
57	Memory of the unjamming transition during cyclic tiltings of a granular pile. Physical Review E, 2005, 72, 051305.	2.1	28
58	Spatio-temporal evolution of rockfall activity from 2007 to 2011 at the Piton de la Fournaise volcano inferred from seismic data. Journal of Volcanology and Geothermal Research, 2017, 333-334, 36-52.	2.1	27
59	Modeling of debris avalanche and generated water waves: Application to real and potential events in Montserrat. Physics and Chemistry of the Earth, 2000, 25, 741-745.	0.6	26
60	A Riemann solver for single-phase and two-phase shallow flow models based on relaxation. Relations with Roe and VFRoe solvers. Journal of Computational Physics, 2011, 230, 515-550.	3.8	26
61	Numerical modeling of a landslide-generated tsunami following a potential explosion of the Montserrat volcano. Physics and Chemistry of the Earth, 1999, 24, 163-168.	0.6	25
62	Complex force history of a calvingâ€generated glacial earthquake derived from broadband seismic inversion. Geophysical Research Letters, 2016, 43, 1055-1065.	4.0	24
63	Toward continuous quantification of lava extrusion rate: Results from the multidisciplinary analysis of the 2 January 2010 eruption of Piton de la Fournaise volcano, La Réunion. Journal of Geophysical Research: Solid Earth, 2015, 120, 3026-3047.	3.4	23
64	On the Link Between External Forcings and Slope Instabilities in the Piton de la Fournaise Summit Crater, Reunion Island. Journal of Geophysical Research F: Earth Surface, 2018, 123, 2422-2442.	2.8	23
65	Link Between the Dynamics of Granular Flows and the Generated Seismic Signal: Insights From Laboratory Experiments. Journal of Geophysical Research F: Earth Surface, 2018, 123, 1407-1429.	2.8	23
66	Location of microseismic swarms induced by salt solution mining. Geophysical Journal International, 2015, 200, 337-362.	2.4	22
67	Experimental validation of theoretical methods to estimate the energy radiated by elastic waves during an impact. Journal of Sound and Vibration, 2016, 362, 176-202.	3.9	22
68	Empirical investigation of friction weakening of terrestrial and Martian landslides using discrete element models. Landslides, 2019, 16, 1121-1140.	5.4	21
69	Elastic wave generated by granular impact on rough and erodible surfaces. Journal of Applied Physics, 2018, 123, 044901.	2.5	18
70	Constraining landslide characteristics with Bayesian inversion of field and seismic data. Geophysical Journal International, 2020, 221, 1341-1348.	2.4	18
71	Monitoring Greenland ice sheet buoyancy-driven calving discharge using glacial earthquakes. Annals of Glaciology, 2019, 60, 75-95.	1.4	17
72	An analytic approach for the evolution of the static/flowing interface in viscoplastic granular flows. Communications in Mathematical Sciences, 2016, 14, 2101-2126.	1.0	17

#	Article	IF	CITATIONS
73	Relations Between the Characteristics of Granular Column Collapses and Resultant Highâ€Frequency Seismic Signals. Journal of Geophysical Research F: Earth Surface, 2019, 124, 2987-3021.	2.8	16
74	A two-phase solid-fluid model for dense granular flows including dilatancy effects: comparison with submarine granular collapse experiments. EPJ Web of Conferences, 2017, 140, 09039.	0.3	15
75	Two-dimensional simulation by regularization of free surface viscoplastic flows with Drucker–Prager yield stress and application to granular collapse. Journal of Computational Physics, 2017, 333, 387-408.	3.8	14
76	Experimental assessment of the effective friction at the base of granular chute flows on a smooth incline. Physical Review E, 2021, 103, 042905.	2.1	13
77	Topography Curvature Effects in Thinâ€Layer Models for Gravityâ€Driven Flows Without Bed Erosion. Journal of Geophysical Research F: Earth Surface, 2021, 126, e2020JF005657.	2.8	13
78	Resolving source mechanisms of microseismic swarms induced by solution mining. Geophysical Journal International, 2016, 206, 696-715.	2.4	12
79	Synthetic benchmarking of concentrated pyroclastic current models. Bulletin of Volcanology, 2021, 83, 1.	3.0	12
80	Triggering granular avalanches with ultrasound. Physical Review E, 2020, 102, 042901.	2.1	11
81	Operational Estimation of Landslide Runout: Comparison of Empirical and Numerical Methods. Geosciences (Switzerland), 2020, 10, 424.	2.2	11
82	A Weakly Non-hydrostatic Shallow Model for Dry Granular Flows. Journal of Scientific Computing, 2021, 86, 1.	2.3	11
83	A Free Interface Model for Static/Flowing Dynamics in Thin-Layer Flows of Granular Materials with Yield: Simple Shear Simulations and Comparison with Experiments. Applied Sciences (Switzerland), 2017, 7, 386.	2.5	10
84	Dynamics of recent landslides (<20 My) on Mars: Insights from high-resolution topography on Earth and Mars and numerical modelling. Planetary and Space Science, 2021, 206, 105303.	1.7	10
85	A two-layer shallow flow model with two axes of integration, well-balanced discretization and application to submarine avalanches. Journal of Computational Physics, 2020, 406, 109186.	3.8	8
86	Analysis of the 2017 June Maoxian landslide processes with force histories from seismological inversion and terrain features. Geophysical Journal International, 2020, 222, 1965-1976.	2.4	8
87	Dilatancy in dry granular flows with a compressible μ(I) rheology. Journal of Computational Physics, 2021, 429, 110013.	3.8	8
88	Laboratory Landquakes: Insights From Experiments Into the Highâ€Frequency Seismic Signal Generated by Geophysical Granular Flows. Journal of Geophysical Research F: Earth Surface, 2021, 126, e2021JF006172.	2.8	8
89	Numerical Modeling of Iceberg Capsizing Responsible for Glacial Earthquakes. Journal of Geophysical Research F: Earth Surface, 2018, 123, 3013-3033.	2.8	7
90	Multilayer models for shallow two-phase debris flows with dilatancy effects. Journal of Computational Physics, 2020, 419, 109699.	3.8	7

#	Article	IF	CITATIONS
91	Numerical Modeling of Two-Phase Gravitational Granular Flows with Bottom Topography. , 2008, , 825-832.		7
92	Simplified simulation of rock avalanches and subsequent debris flows with a single thin-layer model: Application to the Prêcheur river (Martinique, Lesser Antilles). Engineering Geology, 2022, 296, 106457.	6.3	7
93	Simulation of Topography Effects on Rockfallâ€Generated Seismic Signals: Application to Piton de la Fournaise Volcano. Journal of Geophysical Research: Solid Earth, 2020, 125, e2020JB019874.	3.4	6
94	Locating Rockfalls Using Inter‣tation Ratios of Seismic Energy at Dolomieu Crater, Piton de la Fournaise Volcano. Journal of Geophysical Research F: Earth Surface, 2021, 126, e2020JF005715.	2.8	6
95	A two-dimensional method for a family of dispersive shallow water models. SMAI Journal of Computational Mathematics, 0, 6, 187-226.	0.0	6
96	Forensic investigations of the Cima Salti Landslide, northern Italy, using runout simulations. Geomorphology, 2018, 318, 172-186.	2.6	5
97	Modelling capsizing icebergs in the open ocean. Geophysical Journal International, 2020, 223, 1265-1287.	2.4	5
98	Explicit solutions to a free interface model for the static/flowing transition in thin granular flows. ESAIM: Mathematical Modelling and Numerical Analysis, 2021, 55, S369-S395.	1.9	4
99	Assessing the effect of lithological setting, block characteristics and slope topography on the runout length of rockfalls in the Alps and on the island of La Réunion. Natural Hazards and Earth System Sciences, 2021, 21, 1159-1177.	3.6	4
100	Numerical approximation of the 3D hydrostatic Navier–Stokes system with free surface. ESAIM: Mathematical Modelling and Numerical Analysis, 2019, 53, 1981-2024.	1.9	3
101	Some analytical solutions for validation of free surface flow computational codes. Journal of Fluid Mechanics, 2021, 913, .	3.4	2
102	High Order Finite Volume Methods Applied to Sediment Transport and Submarine Avalanches. , 2008, , 247-258.		2
103	A bed pressure correction of the friction term for depth-averaged granular flow models. Applied Mathematical Modelling, 2022, 106, 627-658.	4.2	2
104	Mesh size selection in a soil-biosphere-atmosphere transfer model. Journal of Environmental Engineering and Science, 2003, 2, 77-81.	0.8	1
105	Application of a Combined Finite Element—Finite Volume Method to a 2D Non-hydrostatic Shallow Water Problem. Springer Proceedings in Mathematics and Statistics, 2017, , 219-226.	0.2	1
106	Seismology and Environment. Encyclopedia of Earth Sciences Series, 2020, , 1-8.	0.1	1
107	Short Note: Precision and Convergence of a Steady Two-Dimensional Ice Sheet Flow Model. Mathematical Geosciences, 2001, 33, 229-237.	0.9	0
108	Seismology and Environment. Encyclopedia of Earth Sciences Series, 2021, , 1655-1661.	0.1	0